

Correlations of multiplexed quantum ghost images and improvement of the quality of restored image*

Dmitriy Balakin¹, Alexander Belinsky¹, and Anatoly S. Chirkin^{1,2,*}

¹M. V. Lomonosov Moscow State University, Faculty of Physics
Leninskie Gory, 1, bld 2, Moscow 119991, Russia

²M. V. Lomonosov Moscow State University, The International Laser Center
Leninskie Gory, 1, bld 62, Moscow 119991, Russia

*Corresponding author e-mail: aschirkin @ rambler.ru

Abstract

The currently used ghost image schemes traditionally involve two-mode entangled light states or incoherent radiation. Here, application of four-mode entangled light states is considered. It is shown that multiplexed ghost images (MGI) formed by four-mode entangled quantum light states have mutual spatial correlations determined by the 8th order field correlation functions. A special algorithm to calculate high-order correlations of Bose operators was developed. We also demonstrate that the accounting of MGI correlations allows us to improve the quality of the restored image of an object when processing MGI by measurement reduction method. Computer modelling of recovery of the image from MGI was carried out. It is established that in the considered example the signal-to-noise ratio of the reduced ghost image is 4.6 times higher than the best signal-to-noise ratio for the ghost images themselves.

Keywords: ghost imaging, measurement reduction, entangled photons.

1 Introduction

When observing a ghost image (GI), information on an object is extracted by measuring the spatial correlation between photons propagating through an object or reflected by it, and photons of reference arm which have not interacted with the object. Object photons are measured by a single-pixel or bucket photodetector that has no spatial resolution, while photons of reference arm are registered by a scanning single-pixel photodetector or CCD matrix. As a result, the spatial correlation function that contains information on the object [1] is measured. By now a number of schemes of spatial images have been suggested and carried out (see reviews [2–4] and works [5–9]). The GI technique was extended to X-ray range in experiments [10, 11], and its application in THz range is discussed in [12]. Recently it was shown [13] that this technique can be applied to reconstruct temporal “images” (information) of rapidly varying signal in telecommunication systems. GI attracts interest in connection with a possibility of simplification of illuminating an object, obtaining the image of an object is possible using even a small number of photons. The important characteristics of restored image are its contrast and its signal-to-noise ratio.

The aim of this work is to show that mutual correlation of multiplexed ghost images (MGI) can be used to improve quality of the restored image by means of measurement reduction method. Restoration

*Published as Balakin, D.A., Belinsky, A. V., Chirkin, A. S. Correlations of multiplexed quantum ghost images and improvement of the quality of restored image // Journal of Russian Laser Research. 2017. Vol. 38, N 2. P. 164–172.

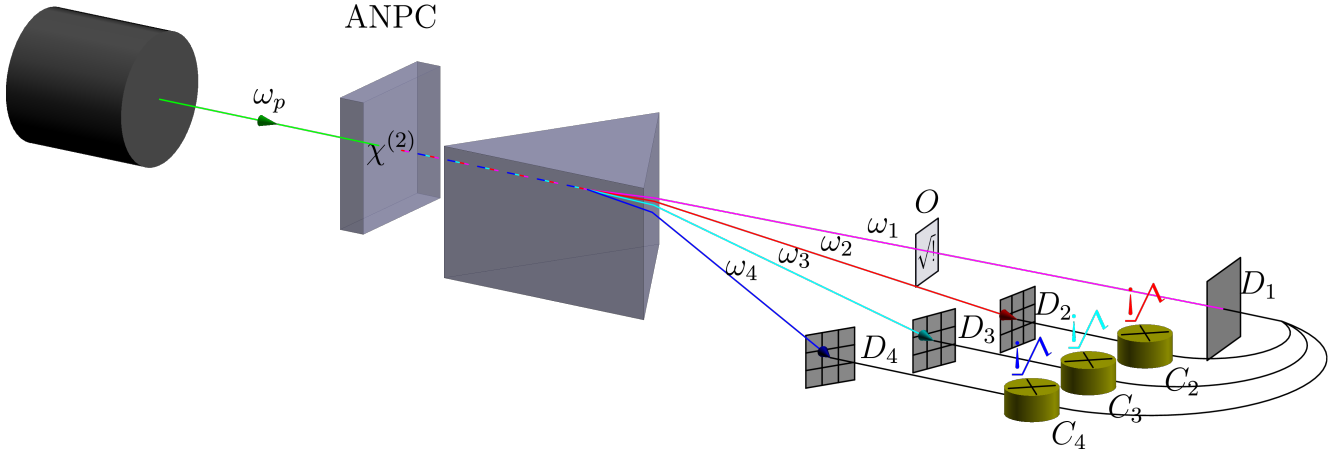


Figure 1: The schematics of set-up of forming multiplied ghost images: ANPC is an aperiodically polarized nonlinear crystal; ω_p is pump frequency; $\omega_1, \dots, \omega_4$ are frequencies of entangled beams that are formed in ANPC; O is the object; D_n are the detectors in object ($n = 1$) and reference ($n = 2, \dots, 4$) arms; C_n are the correlators

and analysis of MGI are illustrated by an example, in which MGI are formed by four-mode entangled quantum light states. It is shown that in this case the signal-to-noise ratio in the restored image can be improved manifold.

2 Multiplexing ghost imaging

The schematics of set-up for obtaining MGI are shown in Fig. 1. Pump radiation, that is, intensive monochromatic radiation with frequency ω_p , falls on an aperiodical nonlinear photon crystal (ANPC). In the crystal, pump photons are split into two photons with frequencies related as

$$\omega_p = \omega_1 + \omega_2.$$

Four-frequency field is obtained as a result of subsequent conversion of a part of photons with frequencies ω_1 and ω_2 into photons with frequencies ω_3 and ω_4 in frequency mixing process:

$$\begin{aligned} \omega_p + \omega_1 &= \omega_3, \\ \omega_p + \omega_2 &= \omega_4. \end{aligned}$$

Effective power exchange between the interacting light waves is carried out if quasi-phase matching condition is satisfied, that is, phase mismatches Δk between the interacting waves are compensated by vectors of the reciprocal aperiodic nonlinear lattices [14, 15]. For example, one can produce four-mode entangled states with wave lengths $\lambda_1 = 2.13 \mu\text{m}$; $\lambda_2 = 1.13 \mu\text{m}$; $\lambda_3 = 0.71 \mu\text{m}$ and $\lambda_4 = 0.53 \mu\text{m}$ if LiNbO_3 ANPC with lattice periods from $8.00 \mu\text{m}$ to $21.20 \mu\text{m}$ is pumped by radiation with wavelength $\lambda_p = 1.06 \mu\text{m}$. It should be noted that the considered process was recently implemented in the scheme with two consistently located nonlinear photon crystals out of the resonator (cascade processes) [16] where the photon pair spectrum at a frequency over the pump frequency was investigated.

Quantum properties of the process under consideration were comprehensively studied in works [17–19], where existence of four-partite entanglement was established. It should be noted that quantum correlations exist not only between photons at low frequencies and between photons at the highest frequencies in relation to pump frequency, but also between low-frequency and high-frequency photons. Some references to other methods of generation of multipartite entangled light fields are given in [6].

In the case of collinear wave interaction geometry, beams after exiting ANPC have to be spatially divided, for example, by a dispersive prism. We denote beam amplitudes operators as $\hat{A}_j(\mathbf{r}, l)$ where the index j corresponds to number of frequency, l is the length of the crystal, and vector \mathbf{r} lies in the plane perpendicular to the propagation direction.

In Fig. 1 the studied object O with transmission coefficient $T(\mathbf{r}_1)$ is lit with the radiation of frequency ω_1 . The detector D_1 registers the light field of the entire beam, and, as noted above, its output does not contain information on spatial transparency distribution of the object. At the same time, information about spatial distribution $T(\mathbf{r}_1)$ is extracted from the measurement of mutual intensity correlations between the object and reference arms [2–4].

The Fourier transform $\hat{a}_j(\mathbf{q})$ (\mathbf{q} is the transverse wave vector) of operators $\hat{A}_j(\mathbf{r})$ at the entrance and at the exit of the nonlinear crystal are related by the expression [17]

$$\hat{\mathbf{a}}(\mathbf{q}, l) = Q(\mathbf{q}, l)\hat{\mathbf{a}}_0(\mathbf{q}, 0), \quad (1)$$

where Q is the 4x4 matrix, elements Q_{mn} of which describe conversion of the field from frequency ω_n to frequency ω_m . Diagonal elements of this matrix describe the conversion of the operator of the field at frequency ω_m . The expression for the matrix Q and its properties are described in [17]. In (1) operators $\hat{\mathbf{a}}$ and $\hat{\mathbf{a}}_0$ are columns of two-dimensional Fourier transforms of spatial creation and annihilation photon operators at the exit and at the entrance of the nonlinear crystal, respectively. The columns are of the form $\hat{\mathbf{a}} = (\hat{a}_1, \hat{a}_2^\dagger, \hat{a}_3, \hat{a}_4^\dagger)^T$, where symbol T means transposing and $\hat{a}_1 = \hat{a}_1(\mathbf{q}, l)$, $\hat{a}_2^\dagger = \hat{a}_2^\dagger(-\mathbf{q}, l)$, $\hat{a}_3 = \hat{a}_3(\mathbf{q}, l)$, $\hat{a}_4^\dagger = \hat{a}_4^\dagger(-\mathbf{q}, l)$.

The amplitude operators of fields in the plane of detectors are related to the operators at the crystal's exit by the following relation:

$$\hat{B}_m(\mathbf{r}_m) = \int H_m(\mathbf{r}_m, \boldsymbol{\rho})\hat{A}_m(\boldsymbol{\rho}, l)d\boldsymbol{\rho}, \quad (2)$$

where $H_m(\mathbf{r}_m, \boldsymbol{\rho})$ is the medium response function related to propagation of the radiation from the crystal to the detector in the m th arm. Note that in (2) we neglected additive operator terms associated with possible losses in the imaging systems (that are necessary to satisfy the commutation relations), as they do not correlate with $A_m(\boldsymbol{\rho})$ and do not contribute to the intensity correlations of interest (see also [4]).

3 Correlations of ghost images

In connection to the stated problem, calculation of the following parameters is necessary:

- the mean value of the intensity operator

$$\langle \hat{I}_m(\mathbf{r}) \rangle = \langle \hat{B}_m^\dagger(\mathbf{r}_m)\hat{B}_m(\mathbf{r}_m) \rangle; \quad (3)$$

- the mutual intensity fluctuation operator

$$\hat{G}_{1i}(\mathbf{r}_1, \mathbf{r}_i) = \hat{I}_1(\mathbf{r}_1)\hat{I}_i(\mathbf{r}_i) - \langle \hat{I}_1(\mathbf{r}_1) \rangle \langle \hat{I}_i(\mathbf{r}_i) \rangle,$$

that is actually the operator of the GI, as its mean value contains information on the object;

- finally, the GI correlation function that is given by

$$G_{1i1j}(\mathbf{r}_1, \mathbf{r}_i, \mathbf{r}'_1, \mathbf{r}_j) = \langle \hat{G}_{1i}(\mathbf{r}_1, \mathbf{r}_i)\hat{G}_{1j}(\mathbf{r}'_1, \mathbf{r}_j) \rangle. \quad (4)$$

Averages of operator expressions are calculated for vacuum state of the field at the entrance of the nonlinear crystal.

The fourth order correlation functions of intensities (4) present the greatest calculation difficulty:

$$\langle \hat{I}_1 \hat{I}_i \hat{I}_1 \hat{I}_j \rangle = \langle \hat{B}_1^\dagger \hat{B}_1 \hat{B}_i^\dagger \hat{B}_i \hat{B}_1^\dagger \hat{B}_1 \hat{B}_j^\dagger \hat{B}_j \rangle.$$

Here and afterwards, arguments of the operators are omitted for brevity.

The average of the product operators in the detector planes (2) expressed through operators at the exit from a crystal has the following form:

$$\begin{aligned} \langle \hat{I}_1 \hat{I}_i \hat{I}_1 \hat{I}_j \rangle = & \int d\rho_1 \int d\rho'_1 \int d\rho_i \int d\rho'_i \int d\rho''_1 \int d\rho'''_1 \int d\rho_j \int d\rho'_j \times \\ & \times H_1^*(\mathbf{r}_1, \boldsymbol{\rho}_1) H_1(\mathbf{r}_1, \boldsymbol{\rho}'_1) H_i^*(\mathbf{r}_i, \boldsymbol{\rho}_i) H_i(\mathbf{r}_i, \boldsymbol{\rho}'_i) \times \\ & \times H_1^*(\mathbf{r}'_1, \boldsymbol{\rho}''_1) H_1(\mathbf{r}'_1, \boldsymbol{\rho}'''_1) H_j^*(\mathbf{r}_j, \boldsymbol{\rho}_j) H_j(\mathbf{r}_j, \boldsymbol{\rho}'_j) \times \\ & \times \langle \hat{A}_1^\dagger(\boldsymbol{\rho}_1) \hat{A}_1(\boldsymbol{\rho}'_1) \hat{A}_i^\dagger(\boldsymbol{\rho}_i) \hat{A}_i(\boldsymbol{\rho}'_i) \hat{A}_1^\dagger(\boldsymbol{\rho}''_1) \hat{A}_1(\boldsymbol{\rho}'''_1) \hat{A}_j^\dagger(\boldsymbol{\rho}_j) \hat{A}_j(\boldsymbol{\rho}'_j) \rangle. \end{aligned}$$

The fields formed by the parametric conversion obey Gaussian statistics, therefore, we can carry out the factorization of $\langle \hat{A}_1^\dagger \hat{A}_1 \hat{A}_i^\dagger \hat{A}_i \hat{A}_1^\dagger \hat{A}_1 \hat{A}_j^\dagger \hat{A}_j \rangle$ using Wick's theorem [20]. According to the theorem, the mean of the product of any number of bosonic creation and annihilation operators over vacuum state is equal to the sum of products of all possible averages of operator pair products, where in each pair factors are ordered the same way as in the initial product. Therefore, the product under discussion is transformed to the sum of terms, each of which is a product of four average products of a pair of operators:

$$\begin{aligned} \langle \hat{A}_1^\dagger \hat{A}_1 \hat{A}_i^\dagger \hat{A}_i \hat{A}_1^\dagger \hat{A}_1 \hat{A}_j^\dagger \hat{A}_j \rangle = & \langle \hat{A}_1^\dagger \hat{A}_1 \rangle \langle \hat{A}_i^\dagger \hat{A}_i \rangle \langle \hat{A}_1^\dagger \hat{A}_1 \rangle \langle \hat{A}_j^\dagger \hat{A}_j \rangle + \dots + \\ & \langle \hat{A}_1^\dagger \hat{A}_1 \rangle \langle \hat{A}_1^\dagger \hat{A}_i \rangle \langle \hat{A}_i^\dagger \hat{A}_j \rangle \langle \hat{A}_1 \hat{A}_j^\dagger \rangle + \dots + \langle \hat{A}_1^\dagger \hat{A}_j \rangle \langle \hat{A}_1 \hat{A}_j^\dagger \rangle \langle \hat{A}_i^\dagger \hat{A}_1 \rangle \langle \hat{A}_i \hat{A}_1^\dagger \rangle. \end{aligned}$$

To carry out this procedure, we have written a program implementing the following algorithm:

1. Operators $\hat{A}_1^\dagger, \dots, \hat{A}_j$ were denoted by numbers $0, \dots, 7$, respectively.
2. From all permutations of the set $\{0, \dots, 7\}$ those which satisfy the following were picked:
 - (a) Each pair of elements of the set obtained by permutation is increasingly ordered.
 - (b) The elements of the set obtained by permutation with odd serial numbers (that is, the first elements of pairs), are increasingly ordered.

Condition 2a is necessary for obtained permutations to satisfy the Wick's theorem conditions, and condition 2b is necessary and sufficient for repeated terms not to appear during factorization.

The factorized product $\langle \hat{A}_1^\dagger \hat{A}_1 \hat{A}_i^\dagger \hat{A}_i \hat{A}_1^\dagger \hat{A}_1 \hat{A}_j^\dagger \hat{A}_j \rangle$ has 105 terms of the form $\langle \hat{A}_k^\dagger \hat{A}_{k'} \rangle, \langle \hat{A}_k \hat{A}_{k'}^\dagger \rangle, \langle \hat{A}_k^\dagger \hat{A}_{k'}^\dagger \rangle$ and $\langle \hat{A}_k \hat{A}_{k'} \rangle$. The result of calculation of $\langle \hat{A}_1^\dagger \hat{A}_1 \hat{A}_i^\dagger \hat{A}_i \rangle \langle \hat{A}_1^\dagger \hat{A}_1 \hat{A}_j^\dagger \hat{A}_j \rangle$ has 9 terms.

To calculate averages $\langle \hat{A}_k^\dagger \hat{A}_{k'} \rangle, \langle \hat{A}_k \hat{A}_{k'}^\dagger \rangle, \langle \hat{A}_k^\dagger \hat{A}_{k'}^\dagger \rangle$ and $\langle \hat{A}_k \hat{A}_{k'} \rangle$, operators \hat{A}_k and \hat{A}_k^\dagger are expressed through operators \hat{a}_k and \hat{a}_k^\dagger by inverse Fourier transformations. Dependence of the latter on the creation and annihilation operators at the crystal's entrance is given by (1). After these actions the factorized expression depends on the Bose operators at the entrance of the crystal, and only averages of products of antinormally ordered operator pairs have nonzero value.

As a result of calculations, taking into account that the detector in the object arm collects radiation from the entire beam aperture and provided that the band of transverse wave numbers of the parametric converter is much larger than the corresponding band of the image, we obtain the expression

$$G_{ij}(\mathbf{r}_i, \mathbf{r}_j) = \left(\frac{k_1}{2\pi f} \right)^4 |T(-\mathbf{r}_i)|^2 |T(-\mathbf{r}_j)|^2 \int \int d\mathbf{r}_1 d\mathbf{r}'_1 W_{ij}(\mathbf{r}_1, \mathbf{r}_i, \mathbf{r}'_1, \mathbf{r}_j), \quad (5)$$

where

$$W_{ij}(\mathbf{r}_1, \mathbf{r}_i, \mathbf{r}'_1, \mathbf{r}_j) = \int d\mathbf{R} \int d\mathbf{d} \int d\mathbf{R}' \int d\mathbf{d}' \exp\left(-i\frac{k_1}{f}(\mathbf{r}_1, \mathbf{d})\right) \exp\left(-i\frac{k_1}{f}(\mathbf{r}'_1, \mathbf{d}')\right) \times \\ \times \widetilde{W}_{ij}(\mathbf{R} - \mathbf{d}/2, \mathbf{R} + \mathbf{d}/2, -\mathbf{r}_i, -\mathbf{r}_i, \mathbf{R}' - \mathbf{d}'/2, \mathbf{R}' + \mathbf{d}'/2, -\mathbf{r}_j, -\mathbf{r}_j).$$

The function \widetilde{W}_{ij} has an extremely cumbersome form. It is determined by the sum of products of Fourier transforms of transfer coefficients $Q_{mn}(q, l)$ in the eighth degree.

Calculation of the correlation function for mutual intensity fluctuations yields the result coinciding with [6]:

$$G_j(\mathbf{r}_j) \stackrel{\text{def}}{=} \int G_{1j}(\mathbf{r}_1, \mathbf{r}_j) d\mathbf{r}_1 = \left(\frac{k_1}{2\pi f}\right)^2 \left| \int Q_{(11j)}\left(\frac{k_1}{f}\mathbf{r}_1\right) d\mathbf{r}_1 \right|^2 |T(-\mathbf{r}_j)|^2, \quad (6)$$

where $Q_{(11j)}(\mathbf{q}) = Q_{11}(\mathbf{q})Q_{j1}^*(\mathbf{q}) + Q_{13}(\mathbf{q})Q_{j3}^*(\mathbf{q})$.

Expressions (5), (6) have been obtained for the case when in the arms of the set-up in Fig. 1 lenses are used (see also [4, 6]). The object and detector D_1 are located in the focal regions of a lens. In the reference arms lenses are located at double focal length from detectors D_j and the crystal. Lenses are not portrayed in Fig. 1.

4 Interpretation of acquired ghost images

We use a two-dimensional array of detectors as a measuring device. The output of each detector is proportional to incoming luminous flux. The values obtained at each correlator's output, denoted as $\xi(\mathbf{r})$, can be represented by the effect on the measuring transducer (MT) on the input signal $f(\mathbf{r}) \sim |T(-\mathbf{r})|^2$. In this article we consider piece-wise constant images, i. e. transparency is constant within each pixel. The algorithm of image interpretation ought to give a maximally accurate estimate of the original image $f(\mathbf{r})$ from the acquired data $\xi(\mathbf{r})$.

Let us represent the measurement model by $\xi(\mathbf{r}) = (Af)(\mathbf{r}) + \nu(\mathbf{r})$, where $f(\mathbf{r})$ is an a priori unknown vector describing the transparency distribution of the measured object; A is the matrix describing the formation and acquisition of ghost images: the matrix element A_{ij} is equal to the mean signal of i -th detector for unit transparency of the j -th object element and zero transparency of other ones; $\nu(\mathbf{r})$ is the noise with zero mean value, corresponding to lack of systematic measurement error, and with covariance matrix $(\Sigma_\nu)_{ij} = \langle \nu(\mathbf{r}_i)\nu(\mathbf{r}_j) \rangle$ that models distortions obtained during flux measurements using the MT. The vector $\xi(\mathbf{r})$ represents the results of flux measurements. The dimension of vector $f(\mathbf{r})$ is given by the number of pixels in the image, and the dimension of the vector $\xi(\mathbf{r})$ is given by the number of the pixels in detector arrays.

Operators A and Σ_ν are related to correlation functions. Since the measurement set-up uses correlators that measure correlations between the first arm and the other arms, MT's effect on the image is given by a block matrix consisting of three blocks representing the correlators' outputs — the correlations of the object arm and the reference arms:

$$A = \begin{pmatrix} B_2 C_2 \\ B_3 C_3 \\ B_4 C_4 \end{pmatrix}, \quad (7)$$

where under conditions given in derivation of (5), (6) matrices C_j are proportional to the identity matrices multiplied by (up to a factor defined by the choice of the measurement units) the pixel size and the factor in front of $|T(\mathbf{r}_i)|^2$ in the expression for G_j (6), and matrices B_j describe the detectors: the matrix element $(B_j)_{pk}$ is equal to the response of the detector at the p -th position in the j -th reference arm to the unit luminance of the k -th pixel and a zero luminance of the other ones.

The noise covariance matrix is a block matrix as well:

$$\Sigma_\nu = \begin{pmatrix} B_2 \Sigma_{22}(f) B_2^* & B_2 \Sigma_{23}(f) B_3^* & B_2 \Sigma_{24}(f) B_4^* \\ B_3 \Sigma_{32}(f) B_2^* & B_3 \Sigma_{33}(f) B_3^* & B_3 \Sigma_{34}(f) B_4^* \\ B_4 \Sigma_{42}(f) B_2^* & B_4 \Sigma_{43}(f) B_3^* & B_4 \Sigma_{44}(f) B_4^* \end{pmatrix}. \quad (8)$$

The element of the block Σ_{ij} with indices k, k' is equal (up to a factor defined by the choice of the measurement units) to the value of integral of G_{ij} over values of \mathbf{r}_i that belong to the k -th pixel and over values of \mathbf{r}_j that belong to k' -th pixel.

The objective of the measurement is to obtain the most accurate estimate of Uf , where operator U describes the ideal measuring transducer, using the measurement data obtained as described above. As show in [21, 22], the linear estimate with the least mean squared error (MSE) is

$$R_* \xi = U(A^* \Sigma_\nu^- A)^- A^* \Sigma_\nu^- \xi, \quad (9)$$

where $^-$ denotes matrix pseudoinverse and R_* is the reduction operator defined by (9). Note that the *mathematical* reduction method is applicable for any other light source — the peculiarity of the described light source is the form of covariance operator Σ_ν that affects step 3 of the processing algorithm given below.

Synthesis of such an estimate is possible if the condition $U(I - A^- A) = 0$ is satisfied, where, as noted above, A described the *real* measuring device, and U describes the *ideal* measurement device with the impulse response function required by the researcher and, consequently, *any required resolution*, if this condition is satisfied. However, usually the higher the desired resolution of the ideal measuring device compared to the real one, the higher the MSE of the synthesized estimate. The specific dependency of the resolution, defined as the maximal rank of U for which estimation of Uf with MSE below given is possible (effective rank, see [21, ch. 8]), depends first and foremost on B_j and the covariance operator of the noise unrelated to ghost imaging. For example, in the case of ideal detectors and white noise this dependency is a linear one — quadruple relaxation of MSE requirement allows to reduce the pixel size by two times.

5 Computer modelling results

For simplicity we consider the case of ideal identical detectors in all the reference arms, $B_2 = B_3 = B_4 = U = I$.

The covariance matrix (8) depends on the unknown input signal. Therefore, the measurement reduction algorithm is an iterative one, with each iteration consisting of three steps:

1. estimation of image using (9) for Σ_ν corresponding to the image with constant transparency and A given by (7) (on the first iteration) or for $\tilde{\Sigma}_\nu = \begin{pmatrix} \Sigma_{\nu,e} & 0 \\ 0 & \kappa I \end{pmatrix}$, $\tilde{A} = \begin{pmatrix} A \\ I \end{pmatrix}$, $\tilde{\xi} = \begin{pmatrix} \xi \\ \hat{f}_e \end{pmatrix}$, where A is given by (7), \hat{f}_e is the image estimate obtained during previous iteration, κ is an arbitrary positive number and $\Sigma_{\nu,e}$ is the estimate of the covariation matrix obtained in the last step of the previous iteration (on later iterations);
2. orthogonal projection of the result onto $[0, 1]^{\dim f}$ to take into account that transparency takes values in $[0, 1]$;
3. substitution of f in (8) by the obtained estimate to refine the estimate of Σ_ν , taking into account that \hat{f}_e and ξ are *correlated*.

The computer modelling results presented in Fig. 2 illustrate an application of above-described processing of MGI. One can see that the image shown in Fig. 2(f) has better quality than the ghost ones

(figures 2(b)–2(d)) and the one (Fig. 2(e)) obtained by summing them up. The simulation was carried out for the following values of parameters: beam wave numbers $k_1 = 6 \cdot 10^4 \text{ cm}^{-1}$, $k_3 = 1.7 \cdot 10^5 \text{ cm}^{-1}$, ANPC parameter $\beta = 10 \text{ cm}^{-1}$, ANPC parameter $\xi = \gamma/\beta = 0.4$, dimensionless ANPC thickness $\zeta = \beta l = 6$. The signal-to-noise ratio for the entire image is 4.6 times higher than the best signal-to-noise ratio for the ghost images themselves, and 7.7 times higher than for their sum if only fluctuations related to ghost imaging are present. The signal-to-noise ratio of the sum of images is different from that of each image due to fluctuations of the images. Therefore, fluctuations in reference arms are partially suppressed by summation, although not to the same degree as if the images were completely uncorrelated. The theoretical change of signal-to-noise ratio in this case is

$$(c_2 + c_3 + c_4)^2 \left((1 \ 1 \ 1) C \begin{pmatrix} 1 \\ 1 \\ 1 \end{pmatrix} \right)^{-1} C_{j_*, j_*} \bar{c}_{j_*}^{-2} \approx 0.6,$$

where, in accordance with formulas for mean and variance of correlated random variables, the first factor is the squared product of unit coefficients with which the images are added and factors $c_2 = 2.73$, $c_3 = 4.98$, $c_4 = 5.11$ in front of identity matrices in C_j in (7), the second factor is the product of the row vector of unit coefficients, the matrix $C = \begin{pmatrix} 0.19 & 0.13 & 0.12 \\ 0.13 & 0.11 & 0.11 \\ 0.12 & 0.11 & 0.11 \end{pmatrix}$ composed of image covariances, and and the column vector of the coefficients, j_* is the number of the ghost image with the best S/N ratio (in this case, the last one). It is in good agreement with the value $4.6/7.7 \approx 0.6$ obtained by computer modelling. In this case summation does not increase the S/N ratio, because large S/N ratio of the first GI offsets the partial suppression of fluctuations by summation.

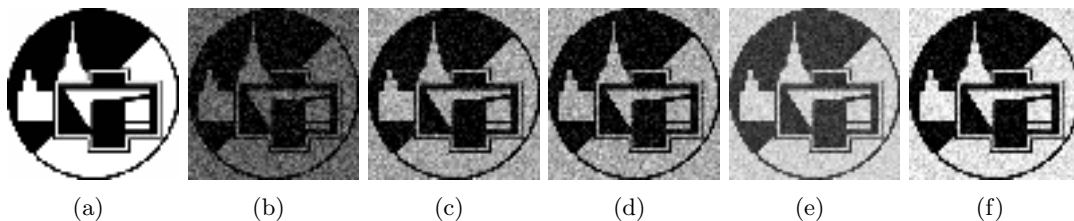


Figure 2: Images of the object acquired using 64x64 pixels array and the result of their reduction: (a) the original image; (b)–(d) acquired ghost images, (e) superposition of ghost images (b)–(d), (f) the result of reduction of ghost images, taking their correlations into account

6 Conclusion

To conclude, we emphasize that the a priori information used for image interpretation consists of ghost image correlation functions. In the considered scheme these correlations are due to the entangled light states produced by the multipartite nonlinear optic process. The computer modelling that was carried out in accordance with developed algorithm showed high efficiency of the proposed method both in sense of improving the image quality and in sense of noise suppression: poorly distinguishable images become easily recognizable after such processing.

An advantage of the suggested MGI scheme over a standard one (without multiplexing) is that several images are obtained simultaneously and frequencies of the object beam and the restoring beams can differ by several octaves. The considered coupled parametric interactions give opportunity to obtain entangled field states between the telecommunication wave length (about $1.50 \mu\text{m}$) and the wavelength (about $0.80 \mu\text{m}$) which is of interest to recording of optical information. Quantum fields with the specified properties can not be obtained by means of one conventional parametric process and beam splitters.

Acknowledgments

The authors are grateful for useful discussion of the work to M. Yu. Saygin and A. P. Shkurinov. This work was supported by RFBR grant N 14-02-00458.

References

- [1] A. V. Belinskii and D. N. Klyshko, *JETP*, **78**:3, 259 (1994).
- [2] J. H. Shapiro and R. W. Boyd, *Quantum Information Processing*, **11**:44, 949 (2012).
- [3] B. I. Erkman and J. H. Shapiro, *Advances in Optics and Photonics*, **2**:4, 405 (2010).
- [4] A. Gatti, E. Brambilla, M. Bache, and L. A. Lugiato, Ghost imaging, In M. I. Kolobov (ed.), *Quantum Imaging*, chapter 5, pages 79–111. Springer, 2007.
- [5] E. D. Lopaeva and M. V. Chekhova, *JETP Letters*, **91**:9, 447 (2010).
- [6] A. S. Chirkin, *JETP Letters*, **102**:6, 404 (2015).
- [7] D.-J. Zhang, H.-G. Li, Q.-L. Zhao, et al., *Phys. Rev. A*, **92**:1, 013823 (2015).
- [8] A. S. Chirkin, *JETP Letters*, **103**:4, 282 (2016).
- [9] Ch.-L. Luo and L.-Q. Zhuo, *Laser Phys. Lett.*, **14**:1, 015201 (2017).
- [10] H. Yu, R. Lu, S. Han, et al., *Phys. Rev. Lett.*, **117**:11, 113901 (2016).
- [11] D. Pelliccia, A. Rack, M. Scheel, et al., *Phys. Rev. Lett.*, **117**:11, 113902 (2016).
- [12] D. W. Youngner, L. M. Lust, and R. W. Boyd, Correlated ghost imager, *US Patent 7767968 B2* (2010).
- [13] P. A. Morris, R. S. Aspden, J. E. C. Bell, et al., *Nature Communications*, **6**, 5913 (2015).
- [14] A. S. Chirkin and I. V. Shutov, *JETP Letters*, **86**:11, 693 (2008).
- [15] A. S. Chirkin and I. V. Shutov, *JETP*, **109**:4, 547 (2009).
- [16] H. Suchowski, B. D. Bruner, Yo. Israel, et al., *Appl. Phys. B*, **122**, 25 (2016).
- [17] M. Yu. Saygin and A. S. Chirkin, *JETP*, **111**:1, 11 (2010).
- [18] T. V. Tlyachev, A. M. Chebotarev, and A. S. Chirkin, *Physica Scripta*, **T160**, 014041 (2014).
- [19] M. Yu. Saygin, *Laser Phys. Lett.*, **13**:10, 105203 (2016).
- [20] V. B. Berestetskii, E. M. Lifshitz, and L. P. Pitaevskii. *Quantum Electrodynamics*, volume 4 of *Course of Theoretical Physics*. Butterworth-Heinemann, 2 ed., 1982.
- [21] Yu. P. Pyt'ev. *Mathematical Modelling Methods of Computer-Aided Measuring Systems [in Russian]*. Fizmatlit, Moscow, 3 ed., 2012.
- [22] D. A. Balakin and A. V. Belinsky. The formation of quantum images and their transformation and super-resolution reading. *JETP*, **122**:5, 787 (2016).